



OPEN

Changes in retinal layers in type 1 diabetes mellitus without retinopathy measured by spectral domain and swept source OCTs

Elvira Orduna-Hospital^{1,2}✉, Ana Sanchez-Cano^{1,2}, Lorena Perdices¹, Javier Acha^{1,3}, Elena María Lopez-Alaminos³ & Isabel Pinilla^{1,4}

To evaluate changes in inner retinal layer (IRL) thicknesses in patients with type 1 diabetes mellitus (DM1) with no diabetic retinopathy (DR) using two different optical coherence tomography (OCT) devices. Ninety DM1 and 60 healthy eyes were evaluated using spectral domain (SD)-OCT and swept source (SS)-OCT to measure changes in the retinal nerve fiber layer (RNFL), ganglion cell layer (GCL), inner plexiform layer (IPL) and inner nuclear layer (INL) thicknesses in all Early Treatment of Diabetic Retinopathy Study (ETDRS) macular areas. Functional tests were performed in both groups, including ETDRS with 100, 2.5 and 1.25% contrast, and color vision. The mean ages were 42.93 ± 13.62 and 41.52 ± 13.05 years in the diabetic and control groups, respectively. Visual acuity (VA) with ETDRS 1.25% was lower in the DM1 patients. Both ETDRS 2.5% and color vision were lower in the DM1 group but did not reach statistical significance. Retinal thicknesses in the central area and in the vertical outer areas were higher in the DM1 group. Differences were found in the IRL with no changes in the outer ones. Long-term DM1 patients with no DR maintained visual function, with a decrease in VA with 1.25% ETDRS contrast. Macular thickness measurements were higher using Spectralis SD-OCT than DRI Triton SS-OCT, and DM1 patients had a decrease in IRL thickness, especially in the GCL at the parafoveal level, generating thinning of the RNFL in the peripheral areas. There were no differences in outer retinal layer (ORL) thickness.

In type 1 diabetes mellitus (DM1) patients, the major cause of visual loss is diabetic retinopathy (DR); before microvascular changes exist, functional changes affect retinal cells. This occurs due to the retinal neurons lost, secondary to a neurodegenerative process. Functional neurodegeneration changes in diabetes have been proven, such as low color perception¹, reduction in contrast sensitivity (CS)², diminished dark adaptation³, abnormal electrophysiological tests⁴, oscillatory potential reduction in the electroretinogram (ERG) or abnormal multifocal pattern ERG⁵; defects in the visual field with concurrent defects in the retinal nerve fiber layer (RNFL) have also been described^{6,7}. The development of optical coherence tomography (OCT) technology permits the quantification of different retinal layer thicknesses and volume changes. This technique allows the visualization of the retinal layers thanks to the refractive properties of each layer, their segmentation and quantification in the Early Treatment of Diabetic Retinopathy Study (ETDRS) macular areas of each retinal layer. By studying changes in the different retinal layers, we identified neurodegeneration.

Several studies have demonstrated a thinning of retinal macular thickness in diabetic patients prior to any sign of DR^{8–10}, mainly due to a diminution of the ganglion cell complex (GCC), comprising the ganglion cell layer (GCL), inner plexiform layer (IPL) and RNFL¹¹. We demonstrated, in a retrospective study with a long follow-up time with Spectralis SD-OCT, inner retinal layer (IRL) diminution in a diabetic population before retinopathy appears¹². Sohn et al.¹³ demonstrated RNFL and GCL-IPL loss during 4 years of follow-up using

¹Aragon Institute for Health Research (IIS Aragon), 50009 Zaragoza, Spain. ²Department of Applied Physics, University of Zaragoza, Pedro Cerbuna, 12, 50009 Zaragoza, Spain. ³Department of Endocrinology, Miguel Servet University Hospital, 50009 Zaragoza, Spain. ⁴Department of Ophthalmology, Lozano Blesa University Hospital, 50009 Zaragoza, Spain. ✉email: elvisabi14@hotmail.com

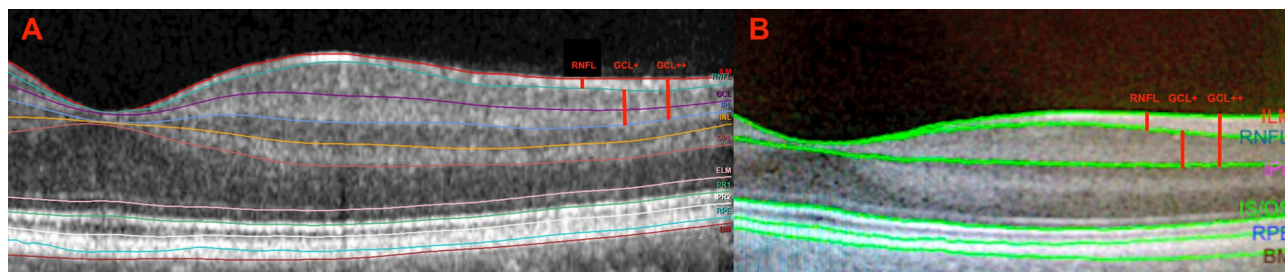


Figure 1. (Tomographic profile obtained by different OCT devices. (A) Tomographic image obtained by Spectralis SD-OCT and automatic segmentation was made by its software version 6.8.1.0. On the right margin are the abbreviations of all the layers of the automated macular segmentation provided by Spectralis SD-OCT software. The thickness of the RNFL, GCL+ and GCL++ protocols are described in the Materials and Methods section. Retinal nerve fiber layer thickness (RNFL) from the inner limiting membrane (ILM) line to the RNFL line. GCL+ thickness from the RNFL line to the inner plexiform layer (IPL) line and GCL++ thickness from the ILM line to the IPL line. GCL, ganglion cell layer; INL, inner nuclear layer; OPL, outer plexiform layer; ELM, external limiting membrane; PR1, photoreceptor inner segments; PR2, photoreceptor outer segments; RPE, retinal pigment epithelium; BM, Bruch membrane. (B) Tomographic image obtained by DRI Triton SS-OCT and automatic segmentation was made by its IMAGENet 6 Version software 1.221.14101 2014 Topcon Corporation. On the right margin are the layer abbreviations of the automated macular segmentation provided by DRI Triton SS-OCT software. The thickness of the RNFL, GCL+ and GCL++ protocols are described in the Materials and Methods section. Retinal nerve fiber layer thickness (RNFL) from the inner limiting membrane (ILM) line to the RNFL line. GCL+ thickness from the RNFL line to the inner plexiform layer (IPL) line and GCL++ thickness from the ILM line to the IPL line. IS/OS, inner/outer segments; RPE, retinal pigment epithelium; BM, Bruch membrane.

Stratus OCT in DM1 patients with no or minimal diabetic lesions and its correlation with animal models and postmortem immunohistochemistry.

The purpose of our study was to assess IRL and outer retinal layer (ORL) thickness changes with two different OCT devices, spectral domain (SD)-OCT and swept source (SS)-OCT, in the macular areas of the ETDRS in DM1 patients without retinopathy compared with a control group and to correlate the thickness results with functional findings measured by visual acuity (AV), CS or color vision in the DM1 group.

Methods

We undertook a prospective study during 2017 including 90 eyes from 90 DM1 patients with no DR and 60 eyes from 60 age-matched healthy subjects. The experimental protocol was approved by the local Ethics Committee for Clinical Research of Aragon (CEICA 18/2017), and the evaluation was conducted in accordance with the principles of the Helsinki Declaration. Detailed consent forms were obtained from each participant.

DM1 patients were controlled by the endocrinology unit. Blood samples were analysed every six months. Glycosylated haemoglobin (HbA1c), lipid values and arterial blood pressure were maintained under extreme control.

The inclusion criteria for the DM1 group were DM1 diagnosis with no retinal changes identified by biomicroscopy or structural OCT; all subjects, the DM1 and the control group, had a best corrected visual acuity (BCVA) over 20/25 on the Snellen chart, with refractive errors between + 5.00 and – 5.00 diopters, normal anterior pole examination with slit-lamp and no funduscopy anomalies. The control group included healthy age-matched subjects to the DM1 group.

Exclusion criteria for both groups were the presence of any sign of DR, glaucoma or intraocular pressure (IOP) over 21 mmHg assessed by Goldman tonometry, optic nerve pathology, ocular inflammation or previous ocular surgery or procedure including laser therapy, ocular traumatism, anterior segment pathology or media opacification.

At each patient's visit, a detailed familiar, systemic and ophthalmological medical history was performed.

The axial length (AL) was measured with the optical biometry *IOLMaster 500* (Carl Zeiss Meditec, Oberkochen, Germany).

Each individual was imaged using a Spectralis SD-OCT¹² (Heidelberg Engineering, Inc., Heidelberg, Germany) and *Deep Range Imaging* (DRI) Triton SS-OCT (Topcon Corporation, Tokyo, Japan). With the Spectralis SD-OCT, the volume fast macula scanning protocol was performed. The subject was asked to look into the internal fixation target, and Tru-Track eye tracking technology was used. Spectralis SD-OCT provides a circular macular map analysis, divided into nine sectorial thickness measurements in three concentric circles with diameters of 1, 3 (inner), and 6 (outer) mm forming the 9 areas corresponding to the ETDRS¹⁴. The central or subfoveal area (1 mm, R1), the 3 mm parafoveal ring with four areas, temporal inner (T1), superior inner (S1), nasal inner (N1), inferior inner (I1), and other four areas belonging to the 6 mm perifoveal ring: temporal outer (T2), superior outer (S2), nasal outer (N2), and inferior outer (I2) to study each macular layer thickness. The Spectralis software version was 6.8.1.0. Once the macular maps were segmented to obtain all retinal layers, the reference lines appeared automatically (Fig. 1); each retinal layer thickness was shown in the ETDRS area. The quality of the scans was checked, and poor-quality scans were rejected. Images should achieve at least 25 over 40 dB. With DRI Triton SS-OCT, a macular 6.0 × 6.0 mm three-dimensional scan was obtained, and automatic segmentation of each retinal layer was made by its IMAGENet 6 Version software 1.22.1.14101 2014 Topcon

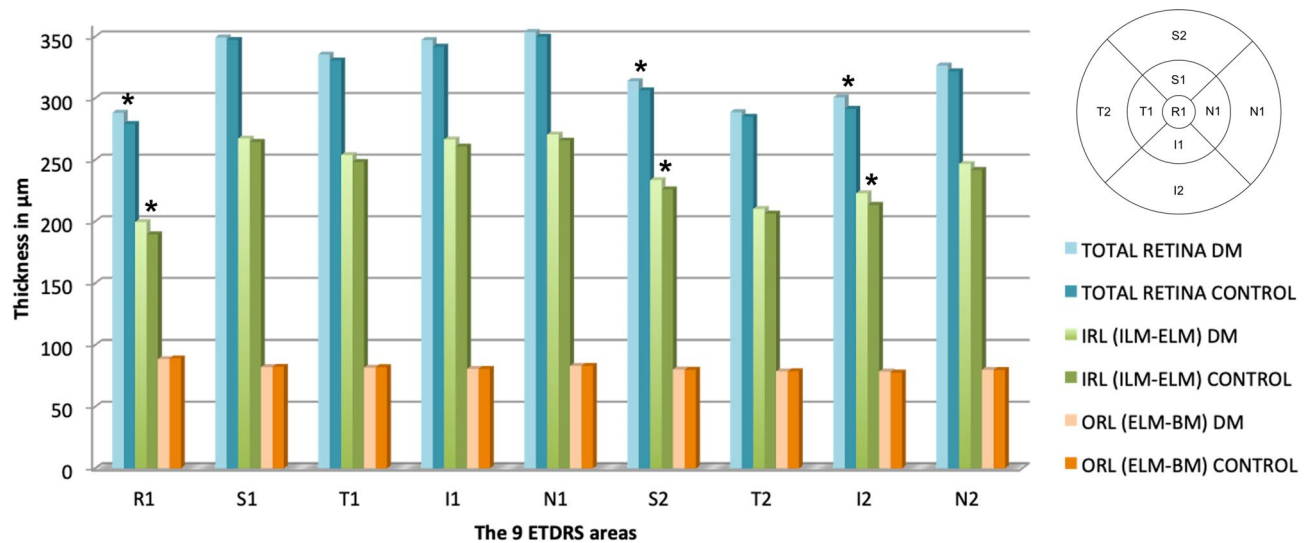


Figure 2. Spectralis SD-OCT measurements. Mean thickness per ETDRS area in μm and statistical significance with $p < 0.05$ marked with * of the total retina, the IRL (from the ILM to the ELM) and the ORL (from the ELM to the BM) in the diabetic and control groups. *DM* Diabetes mellitus, *ETDRS* Early Treatment of Diabetic Retinopathy Study, *ILM* Internal limiting membrane, *ELM* External limiting membrane, *BM* Bruch membrane, *IRL* Inner retinal layers, *ORL* Outer retinal layers, *R1* Central, *S* Superior, *T* Temporal, *I* Inferior, *N* Nasal, 1 corresponds to the values of the 3 mm parafoveal inner circle, and 2 corresponds to the values of the 6 mm peripheral outer circle.

Corporation (Fig. 1). DRI Triton SS-OCT includes the new SMARTTrack tool that enhances tracking, corrects for motion, and guides the operator to reduce potential errors while acquiring the images. Only eyes with good-quality scans defined as those with a signal strength $\geq 70/100$ and without motion artefacts, involuntary saccades, or overt misalignment of decentration were included. DRI Triton SS-OCT provides the same circular macular map analysis as Spectralis SD-OCT, which is composed of the 9 areas corresponding to the ETDRS.

The Spectralis SD-OCT segments all the layers of the retina in the IRL and ORL. It also divides the IRL into 6 layers, the RNFL, the GCL, the IPL, the inner nuclear layer (INL), the outer plexiform layer (OPL) and the outer nuclear layer (ONL), which are the ones analysed in this study (Fig. 1).

The DRI Triton SS-OCT segments only part of the IRL, giving values of the RNFL, the GCL+, which includes the GCL and the IPL, and the GCL++, which includes the GCC (RNFL, GCL and the IPL) (Fig. 1).

To compare the DRI Triton SS-OCT measurements with the Spectralis SD-OCT measurements, we used DRI Triton SS-OCT protocols: the RNFL, GCL+ and GCL++. We calculated the GCL+ thickness as the sum of the GCL and the IPL obtained by Spectralis SD-OCT, and the GCL++ was the sum of the values of the RNFL, the GCL and the IPL.

The exams with both OCT systems were performed on the same day and between 1:00 p.m. and 4:00 p.m. A single well-trained technician obtained all OCT images.

The measurements of the variables to be studied were recorded in an Excel database (Microsoft Office Excel 2011, Microsoft Corporation) and also the elaboration of Figs. 2, 3, 4 and 5. Statistical analysis was performed using the Statistical Package for the Social Sciences (SPSS 20, SPSS Inc., IBM Corporation, Somers, NY, USA). Normal distribution of the values was studied with the Kolmogorov–Smirnov test. As they did not have a normal distribution, the non-parametric Kolmogorov–Smirnov test was used to compare variables of the thickness of the different retinal layers between the two independent groups, such as the control group and the DM1 group. A p value < 0.05 was considered statistically significant.

Ethics declarations. The experimental protocol was approved by the local Ethics Committee for Clinical Research of Aragon (CEICA 18/2017), and the evaluation was conducted in accordance with the principles of the Helsinki Declaration.

Consent to participate. Detailed informed consent forms were obtained from each participant.

Consent to publish. Consent for publication was given by each author and participant.

Results

The mean age of the 90 DM1 patients was 41.52 ± 13.05 years (22–65) and 42.41 ± 13.56 years (26–68) for the 60 healthy controls, without age differences ($p = 0.361$). DM1 patients were well controlled, with a mean glycosylated haemoglobin (HbA1c) of $7.76 \pm 1.06\%$. The mean DM1 evolution time was 24.88 ± 8.42 years (range 9–40 years).

Both groups had no differences in their AL ($p = 0.908$), anterior chamber depth (ACD) ($p = 0.999$) or refractive errors ($p = 0.394$).

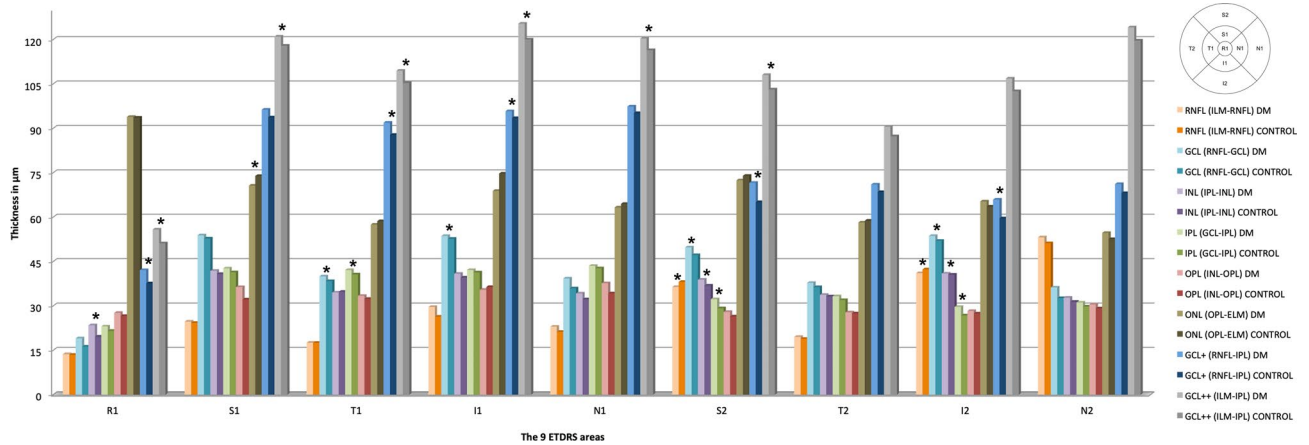


Figure 3. Spectralis SD-OCT mean thickness per ETDRS area is in μm , and statistical significance with $p < 0.05$ is marked with * of the RNFL (from the ILM to the RNFL), GCL (from the RNFL to the GCL), IPL (from the GCL to the IPL), INL (from the IPL to the INL), OPL (from the INL to the OPL), ONL (from the OPL to the ELM), GCL+ (from the RNFL to the IPL, adding GCL and IPL) and GCL++ (GCC) in the diabetic and control groups. *DM* Diabetes mellitus, *ETDRS* Early Treatment of Diabetic Retinopathy Study, *RNFL* Retinal nerve fiber layer, *ILM* Inner limiting membrane, *GCL* Ganglion cell layer, *IPL* Inner plexiform layer, *INL* Inner nuclear layer, *OPL* Outer plexiform layer, *ONL* Outer nuclear layer, *ELM* External limiting membrane, *R1* Central, *S* Superior, *T* Temporal, *I* Inferior, *N* Nasal, 1 corresponds to the values of the 3 mm parafoveal inner circle, and 2 corresponds to the values of the 6 mm peripheral outer circle.

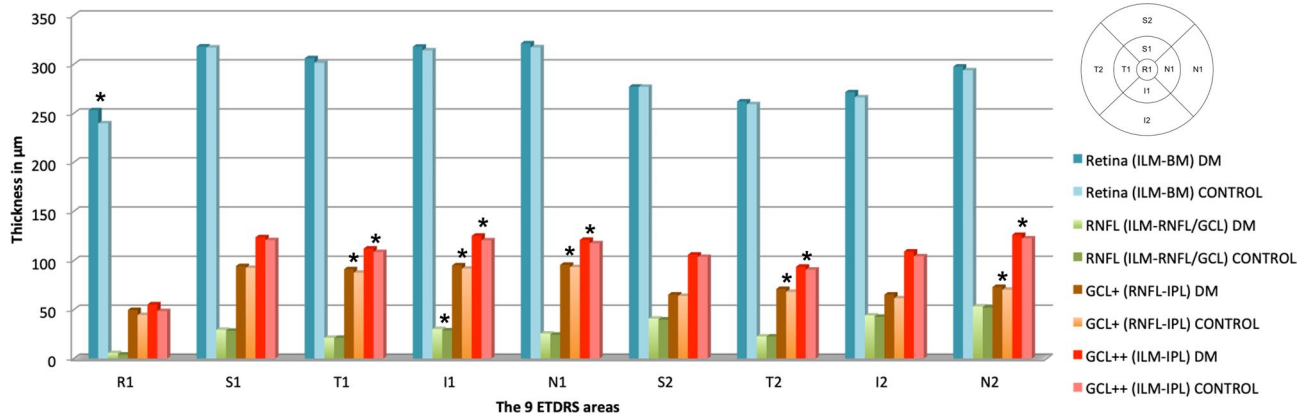


Figure 4. DRI Triton SS-OCT. Mean thickness per ETDRS area is in μm , and statistical significance with $p < 0.05$ is marked with * of the total retina (from the ILM to the BM), RNFL (from the ILM to the RNFL), GCL+ (from the RNFL to the IPL) and GCL++ (from the ILM to the IPL) in the diabetic group and in the control group. *DM* Diabetes mellitus, *ETDRS* Early Treatment of Diabetic Retinopathy Study, *RNFL* Retinal nerve fiber layer, *GCL* Ganglion cell layer, *BM* Bruch membrane, *ILM* Inner limiting membrane, *IPL* Inner plexiform layer, *R1* Central, *S* Superior, *T* Temporal, *I* Inferior, *N* Nasal, 1 corresponds to the values of the 3 mm parafoveal inner circle, and 2 corresponds to the values of the 6 mm peripheral outer circle.

Functional results. BCVA taken with ETDRS tests for 100% contrast was very similar between the two groups ($p = 0.91$). When assessing the ETDRS with a 2.5% contrast, the BCVA in the DM1 group had lower values without reaching statistically significant differences ($p = 0.24$), but in the ETDRS with a contrast of 1.25%, statistically significant differences were found ($p = 0.03$), with the lowest BCVA in the DM1 group. In the color vision evaluation with the Farnsworth-Munsell 15D CVR test, worse results were observed in the DM1 group, but within the normal limits and with no differences in any of the indexes (Table 1).

SD-OCT results. Comparing total retinal thickness between the DM1 group and the control group measured by Spectralis SD-OCT and its macular protocol, we only found differences in the central area ($R1$, $p = 0.030$) and the vertical perifoveal areas ($S2$: $p = 0.004$ and $I2$: $p = 0.009$, respectively), with greater thicknesses in the DM1 group. The $R1$ thickness values were $288.28 \pm 28.59 \mu\text{m}$ vs $279.28 \pm 16.36 \mu\text{m}$ in the DM1 group vs control group, respectively. In the $S2$ area, the values were $313.91 \pm 20.65 \mu\text{m}$ and $306.57 \pm 16.07 \mu\text{m}$ in the DM1 group and control group, respectively, and in the $I2$ area, the values were $300.76 \pm 22.68 \mu\text{m}$ vs $291.37 \pm 14.81 \mu\text{m}$ in the DM1 group and control group, respectively. Dividing the retina into internal (IRL) and external (ORL) layers, we

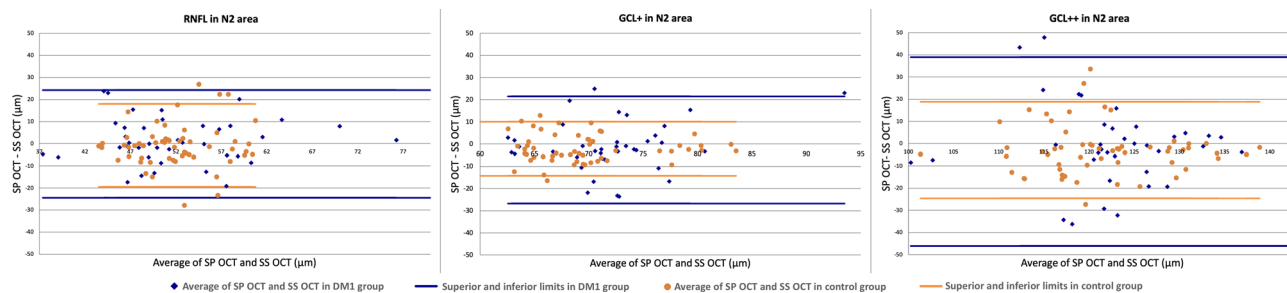


Figure 5. Bland–Altman plots for the RNFL (from the ILM to the RNFL), the GCL+ (from the RNFL to the IPL) and the GCL++ (from the ILM to the IPL) average thickness between SD-OCT and SS-OCT in the nasal outer area N2. In each plot, corresponding layer is represented for the DM1 group in blue and for the control group in orange. *RNFL* Retinal nerve fiber layer, *GCL* Ganglion cell layer, *ILM* Inner limiting membrane, *IPL* Inner plexiform layer, *SD-OCT* Spectral domain optical coherence tomography, *SS-OCT* Swept source optical coherence tomography.

		Control group (mean ± SD)	DM patients (mean ± SD)	<i>p</i>
BCVA (logMAR)	ETDRS at 100%	− 0.113 ± 0.097	− 0.13 ± 0.11	0.91
	ETDRS at 2.5%	+ 0.21 ± 0.18	+ 0.35 ± 0.16	0.24
	ETDRS at 1.25%	+ 0.32 ± 2.27	+ 0.35 ± 2.87	0.03*
IOP (mmHg)		16.59 ± 2.27	16.82 ± 2.87	0.15
Farnsworth Munsell Color Test 15D	CCI	1.00 ± 0.00	1.04 ± 0.13	0.98
	AC CCI	1.00 ± 0.00	1.03 ± 0.19	0.98
	C-index	1.00 ± 0.00	1.05 ± 0.19	0.86
	S-index	1.48 ± 0.00	1.49 ± 0.09	0.98
	Confusion angle	61.5 ± 0.00	61.73 ± 7.68	0.98

Table 1. Mean and standard deviation (SD) of the visual function parameters obtained in the control group and in DM1 patients and their comparison (*p* value). The differences that reached statistical significance (*p* < 0.05) are indicated with *. *DM1* Diabetes mellitus, *SD* Standard deviation, *BCVA* Best corrected visual acuity, *IOP* Intraocular pressure, *ETDRS* Early Treatment of Diabetic Retinopathy Study, *CCI* Color confusion index, *AC-CCI* Age-corrected color confusion index, *C-index* Confusion index, *S-index* Selectivity index.

observed that in the three described areas (R1, S2 and I2), these differences belonged to the IRL, with no changes in the ORL thicknesses (Fig. 2).

We studied each IRL layer to evaluate the observed differences, including the RNFL, GCL, IPL, INL, OPL and ONL in the different ETDRS areas (Fig. 3). The majority of these retinal layer thickness values were higher in the DM1 group than in the controls, but the differences were observed in the IRL in the central area (R1) belonging mostly to the INL (*p* = 0.003), where there are only cones or Müller cell nuclei.

In the vertical peripheral areas (S2 and I2), we observed that the IRL differences reached statistical significance in the four innermost layers. We found thickness differences in the RNFL (S2, *p* = 0.012; I2, *p* = 0.044), GCL (S2, *p* < 0.001; I2, *p* = 0.002), IPL (S2, *p* = 0.004; I2, *p* = 0.023) and INL (S2, *p* = 0.003; I2, *p* < 0.001).

The GCL was the layer with higher differences between groups observed in the inner parafoveal ring, where their cell bodies are located. The T1 and I1 areas had higher thicknesses in the DM1 group (T1: 39.98 ± 4.58 μm vs 38.38 ± 4.00 μm with *p* < 0.001 and I1: 53.62 ± 5.99 μm vs 52.67 ± 4.41 μm with *p* = 0.030, in DM1 patients vs controls, respectively). However, there were no differences in the ONL between the groups. Differences were also found in the S1 area of the OPL (*p* < 0.001) and in the T1 area of the IPL (*p* = 0.014), with higher values in the DM1 patients (Fig. 3).

Calculating GCL+ and GCL++ with Spectralis SD-OCT, differences were found in the GCL+ in the R1 (*p* = 0.011), T1 (*p* < 0.001), I1 (*p* = 0.024), S2 (*p* < 0.001) and I2 (*p* < 0.001) areas. For GCL++, the only areas with no differences were the peripheral T2 (*p* = 0.273), I2 (*p* = 0.190) and N2 (*p* = 0.162) areas (Fig. 3).

SS-OCT results. Total retinal thickness using the DRI Triton SS-OCT had significant differences at the central area (R1), achieving values of 253.11 ± 28.36 μm vs 239.77 ± 22.91 μm in DM1 vs control (*p* = 0.014), respectively, which were the highest values in the DM1 group as already described with Spectralis SD-OCT. The values obtained with Spectralis SD-OCT were 30–40 μm higher than those obtained with DRI Triton OCT. However, unlike the results obtained with the Spectralis SD-OCT, for DRI Triton SS-OCT, there were no statistically significant differences in either S2 or I2 areas.

When studying the RFNL with DRI Triton SS-OCT, differences were observed in the I1 area with values of $30.20 \pm 3.70 \mu\text{m}$ vs $28.78 \pm 2.04 \mu\text{m}$ in the DM1 group vs the control group, respectively ($p = 0.016$), where it is barely thick and probably due to the high standard deviation present in the DM1 group (Fig. 4).

Using the GCL+ and GCL++ protocols, statistically significant differences were observed in all 3 mm ring areas except S1.

When studying the 6 mm perifoveal ring with both protocols, we found significant differences in the horizontal areas of the GCL+ (T2, $71.13 \pm 7.85 \mu\text{m}$ vs $68.21 \pm 6.52 \mu\text{m}$, $p = 0.017$ and N2: $73.08 \pm 9.35 \mu\text{m}$ vs $70.25 \pm 6.49 \mu\text{m}$, $p = 0.004$ in the DM1 and control groups, respectively) and in the GCL++ (T2, $93.75 \pm 9.12 \mu\text{m}$ vs $90.77 \pm 7.50 \mu\text{m}$, $p = 0.017$ and N2: $126.29 \pm 14.54 \mu\text{m}$ vs $122.55 \pm 9.83 \mu\text{m}$, $p = 0.004$, in the DM1 and control groups, respectively).

SD-OCT versus SS-OCT results. To compare the DRI Triton SS-OCT measurements with the Spectralis SD-OCT measurements, we used DRI Triton SS-OCT protocols: the RNFL, GCL+ (sum of GCL and IPL with Spectralis SD-OCT) and GCL++ (sum of RNFL, GCL and IPL with Spectralis SD-OCT). We did not find the same differences with both devices, especially in the values of the RNFL and in the outer ring values (Figs. 3, 4).

The RNFL thickness values were the ones with the highest differences between the two devices ($p < 0.001$). The studied layers had very low thickness values, making segmentation difficult. These differences disappeared closer to the optic nerve in the nasal perimacular areas in both groups (N2: $p = 0.792$ in controls and $p = 0.512$ in DM1) since the RNFL reached its greatest thickness.

The GCL+ and GCL++ values in the control group were quite similar between the two OCT systems, with differences only in the R1 ($p < 0.001$) and I2 areas ($p = 0.024$) of the GCL+ and in both temporal quadrants (T1: $p = 0.004$ and T2: $p = 0.014$) for the GCL++; in both protocols, the thicknesses were higher with DRI Triton SS-OCT. In the DM1 group, we found differences in GCL+ and GCL++ between devices in a greater number of areas. For the GCL+, we obtained differences in R1 ($p < 0.001$) and in all peripheral areas (S2: $p < 0.001$, I2: $p = 0.037$ and N2: $p = 0.012$), except in the temporal area (T2: $p = 0.825$). In contrast, in the GCL++ containing the RNFL, differences were observed in all the peripheral quadrants (S2: $p < 0.001$, T2: $p = 0.001$, I2: $p < 0.001$ and N2: $p < 0.001$) and in two of the parafoveal quadrants (T1: $p < 0.001$ and I1: $p < 0.001$) with thicker thicknesses in this layer with the DRI Triton SS-OCT. All the differences that reached statistical significance for the three protocols in the control group were repeated in the DM1 group.

Figure 5 shows the measurements of each layer and in the same area taken by both devices. The comparison found predominantly agreements between the two OCTs.

Discussion

In our study, we only found differences in visual function in the BCVA measurement with a contrast of 1.25% ($p = 0.030$). The BCVA with 100% contrast in our DM1 group without DR was good ($-0.13 \pm 0.11 \log\text{MAR}$, $p = 0.910$), better than the BCVA found by Zhu et al. ($0.10 \pm 0.19 \log\text{MAR}$) in DM2; they also found no differences with the control group¹⁵. In another follow-up study, the initial BCVA in DM1 patients was $-0.03 \pm 0.16 \log\text{MAR}$ but worsened to $0.03 \pm 0.20 \log\text{MAR}$ 10 years later¹⁶. Good BCVA values were related to the mean age of the DM1 group (41.52 ± 13.05 years) and with acceptable glycaemic control (HbA1c, $7.76 \pm 1.06\%$)¹⁷.

In patients with DR in DM1 and DM2, there is a decrease in CS, which may be independent of the involvement of VA^{2,15}, but there is no agreement on whether this involvement begins before DR; if so, this fact would support an early degeneration of retinal neurons. Several studies found a decrease in CS in DM1 and DM2 without DR for all spatial frequencies, with higher differences while increasing the spatial frequency^{2,3,18}. It has been suggested that the selective loss of the CS for higher frequencies could be a sign of parvocellular pathway dysfunction¹, which comprises 80% of the ganglion cells that are responsible for contrast transmission and color¹⁹.

Regarding color vision, in our study, we did not find differences between groups in any of the Farnsworth-Munsell 15D test indexes. Numerous studies have detected the presence of defects in the color vision of DM1 and DM2 patients with DR in the blue-yellow axis (tritanopia)^{20,21}. Color vision defects have also been described in DM1 and DM2 without DR^{1,22}, suggesting that it may be an early manifestation of the neuronal dysfunction of DM, with cone effects in the absence of visible microvascular changes^{23,24}.

OCT has become an important tool to study the retina in DM patients in early stages and to control the changes that occur therein throughout the disease²⁵. In some of the studies in diabetic patients using OCT, there seemed to be retinal thickening as an early DR sign, without the existence of diabetic macular oedema^{25,26}. Retinal thickness variations could be related to modifications in the blood-retinal barrier^{27–29}, changes in vascular pericytes and endothelial cells^{27,30}, or in glial cells, preferably Müller cells. Other studies have demonstrated neuroglial modification caused by sustained hyperglycaemia^{27,31,32}, with different suggestions; some authors discuss that there may be neuroglial loss with a decrease in layer thickness³², or on the contrary, Müller cell hyperreactivity with an increase in central area thickness³³.

In our study, the average total retinal thickness in the 9 ETDRS areas was thicker in the DM1 patients than that in the control group. Lattanzio et al. reported similar results, with a thickness increase measured with OCT in both DM1 and DM2 patients, being thicker with the DR degree, but they did not review the time of DM evolution or metabolic control³⁴. The thickness increase once the DR is established is a proven fact given the diffusion from the vessels due to the rupture of the internal blood-retinal barrier, causing macular damage^{27–29}.

We found thickness differences in the total retina with Spectralis SD-OCT between the control and the DM1 group in the central area (R1, $p = 0.030$) and in vertical perifoveal areas (S2, $p = 0.004$ and I2, $p = 0.009$). With the DRI Triton SS-OCT, we also found differences in the central area (R1, $p = 0.014$), with DM1 values higher than those of the control group. Sanchez-Tocino et al.²⁶ studied DM patients without DR with similar characteristics and found an increase in the central area (R1) of the DM group. These authors also comment that there were no

differences in any of the macular parameters of their study between patients without DR and patients with DR without clinically significant diabetic macular oedema. Dhasmana et al. found a higher foveal thickness in DM2 patients with DR compared to those without DR and thicker foveal thickness than the control group without reaching differences between patients without DR and healthy subjects³⁵.

The fovea (R1) recorded the lowest thickness with both devices, in addition to the greater thickness difference between groups in the total retina (differences between DM1 and controls of 9 μm and 13.34 μm in Spectralis SD-OCT and DRI Triton SS-OCT, respectively, superior for the DM1 group) followed by the peripheral temporal (T2) ones.

Retinal thickness was higher with Spectralis SD-OCT than with DRI Triton SS-OCT, which is related to their differences in their established limits. With Spectralis SD-OCT, retinal delimitation reaches the BM, while DRI Triton SS-OCT delimits the retina to the upper limit of the RPE^{36,37}. Other factors are their differences in technologies, wavelengths and software^{38,39}. It would be convenient to incorporate a conversion formula for comparing thickness measurements with different OCTs⁴⁰.

We found that the total retinal areas measured by Spectralis SD-OCT that showed differences were justified by changes in the IRL (R1, S2 and I2), while no modifications were found in the ORL thicknesses (Fig. 2). Ciresi et al.⁴¹ also found an increase in thickness in DM1 without DR in both the central (R1) and 6 mm peripheral areas. We segmented and compared each layer separately, and we only found differences in the INL central area (R1) ($p = 0.003$). There are different reasons that justify these findings, such as some inclination in the tomographic image, segmentation error due to the low thickness values at this level and the difficulty of manual modifications or changes at Henle's fiber layer because at this level, we only have photoreceptors and Müller cell nuclei.

Looking at the 3 mm parafoveal ring and analysing the different IRL layers with Spectralis SD-OCT, the differences in T1 and I1 belong to the GCL. Regarding the GCL-IPL and GCC, we found differences in the 3 mm parafoveal ring in the T1, I1 and N1 areas with both protocols and with both devices (excluding N1 for DRI Triton OCT). The ganglion cell bodies are located in this 3 mm ring, and if there are modifications in the GCL, thickness changes will occur here.

For the 6 mm perifoveal ring with Spectralis SD-OCT, the differences between the DM1 and the control group were observed in the vertical areas (S2 and I2) in the four innermost layers: RNFL, GCL, IPL and INL. We again objectify the low thickness values of all these layers; the RNFL is mainly located in the 6 mm peripheral circle where it can undergo major thickness changes.

There were significant differences between groups with DRI Triton SS-OCT, in the 6 mm peripheral ring, and in the horizontal areas for both GCL+ and GCL++ protocols.

Analysing the results obtained by both devices in each group, we found important thickness differences, especially in the RNFL thickness values, with statistical significance in 8 of the 9 ETDRS areas. These differences disappeared in the peripheral nasal area (N2), where the RNFL reaches its greatest thickness close to the optic nerve in both groups. Therefore, the RNFL values are not comparable for both OCT systems and are more reliable when thickness values increase. Both GCL-IPL and GCC were quite similar between the two OCT systems. Only significant differences were obtained for the GCL+ in R1 and I2 and for the GCL++ in both temporal areas (T1 and T2). This fact suggests that although layers are analysed in an individual way, there are differences between them when values increase, and these differences tend to disappear, as already described with the RNFL thickness. We found more differences in the DM group in the GCC, including the RNFL, with both protocols (GCL+ and GCL++), and for both groups, larger thicknesses were found with DRI Triton SS-OCT than Spectralis SD-OCT. With these data, we can speculate that the GCL+ and the GCL++ could be compared between OCT devices in healthy subjects, since the differences are minimal, but in pathological patients caution is necessary since the alterations in the different retinal layers can be segmented differently with each OCT giving differences in more ETDRS areas when comparing the values.

The superior RNFL loss in diabetic patients has also been attributed to less perfusion in the superior retina and optic nerve head, which could generate greater ischaemia that structurally damages ganglion cells⁴².

Histological studies have identified highly suggestive retinal neurodegeneration changes (loss in RNFL and GCL and increase in glial cells) in animal models or in postmortem studies of diabetic donors^{13,43}.

This study demonstrates that in DM1, the GCL is vulnerable to progressive damage before the appearance of microvascular DR. We found some studies in DM1 and DM2^{44–47} in which subjects with moderate or severe DR had a thinner GCL than subjects without DR. Vujosevic et al.⁴⁸ found this same decrease in GCL in DM1 and DM2 subjects who had no obvious DR lesions, which was reflected in thinning at the RNFL level. Vujosevic et al. using DRI-triton OCT, and after adjusting for age and DM duration⁴⁹, found that GCL+ (49.4 μm vs. 43.6 μm , $p = 0.0099$) and GCL++ complex (57.2 μm vs. 50.5 μm , $p = 0.0367$) thicknesses in R1 were significantly higher in patients with DM1 than in patients with DM2 without DR, but in both DM groups were thinner than controls; GCL++ complex in the inner ring was thinner in patients with DM versus controls. Srinivasan et al.⁵⁰, using SD-OCT, found that DM2 patients had significantly reduced full retinal thickness in the parafovea and perifovea and the reduction of the RNFL and GCC thickness was higher than DM1 patients. Scarinci et al.⁵¹, recently reported a thinning of the GCL layer in patients with DM1 and no DR with SD-OCT. The exact mechanisms for IRL thickness loss, a fact revealed in our study after 8 years of evolution in the same sample of DM1 patients¹² and compatible with the neurodegeneration theory, are not clear but have been related to less perfusion and higher metabolic demands of the internal retina that make it more vulnerable to diabetes-induced metabolic stress⁴⁴. Other factors could modify the retinal structure, RNFL thinning has been attributed to the microvascular changes such as leukostasis, vascular obliterations, changes basal membrane^{52–54}. Homocysteine levels have a positive correlation with the thinning of the RNFL⁵⁵. Thinning of the RNFL has also been correlated with the severity of the disorganization of the inner retinal layers (DRIL) in diabetic patients⁵⁶ and an increase of serum levels of VEGF or ICAM1 have been related to the degree of the DR or the disruptions in the ELM and ellipsoid zone⁵⁷.

We did not find ONL differences between groups measured with Spectralis SD-OCT.

In conclusion, long-term DM1 patients with no DR signs maintained visual function, except for a loss in 1.25% ETDRS contrast. Both Spectralis SD-OCT and DRI Triton SS-OCT can detect changes in the macular thickness of the different retinal layers.

Patients with DM1 without DR have thickness changes in the IRL measured in the ETDRS areas, especially in the ganglion cell bodies located in the GCL at the parafoveal level, generating damage of the RNFL in the peripheral areas. This RNFL thinning and the retinal neurodegeneration could be a possible strategy for treating DM patients slowing down the development of the DR.

There were no differences between controls and diabetic patients in ORL at the macular level. New studies on changes at the structural OCT level and other changes such as modifications at the OCTA level are necessary to confirm and justify this finding.

Data availability

All the necessary data are included in the manuscript.

Received: 20 January 2021; Accepted: 5 May 2021

Published online: 17 May 2021

References

- Ewing, F. M., Deary, I. J., Strachan, M. W. & Frier, B. M. Seeing beyond retinopathy in diabetes: electrophysiological and psychophysical abnormalities and alterations in vision. *Endocr. Rev.* **19**, 462–476. <https://doi.org/10.1210/edrv.19.4.0340> (1998).
- Sokol, S. *et al.* Contrast sensitivity in diabetics with and without background retinopathy. *Arch. Ophthalmol.* **103**, 51–54 (1985).
- Ismail, G. M. & Whitaker, D. Early detection of changes in visual function in diabetes mellitus. *Ophthalmic Physiol. Opt.* **18**, 3–12 (1998).
- Mariani, E., Moreo, G. & Colucci, G. B. Study of visual evoked potentials in diabetics without retinopathy: correlations with clinical findings and polyneuropathy. *Acta Neurol. Scand.* **81**, 337–340 (1990).
- Di Leo, M. A. *et al.* Spatial frequency-selective losses with pattern electroretinogram in type 1 (insulin-dependent) diabetic patients without retinopathy. *Diabetologia* **33**, 726–730 (1990).
- Abrishami, M., Daneshvar, R. & Yaghubi, Z. Short-wavelength automated perimetry in type I diabetic patients without retinal involvement: a test modification to decrease test duration. *Eur. J. Ophthalmol.* **22**, 203–209. <https://doi.org/10.5301/EJO.2011.8364> (2012).
- Pinilla, I. *et al.* Changes in frequency-doubling perimetry in patients with type I diabetes prior to retinopathy. *Biomed. Res. Int.* **2013**, 341269. <https://doi.org/10.1155/2013/341269> (2013).
- Chihara, E., Matsuoka, T., Ogura, Y. & Matsumura, M. Retinal nerve fiber layer defect as an early manifestation of diabetic retinopathy. *Ophthalmology* **100**, 1147–1151 (1993).
- Bronson-Castain, K. W. *et al.* Early neural and vascular changes in the adolescent type 1 and type 2 diabetic retina. *Retina* **32**, 92–102. <https://doi.org/10.1097/IAE.0b013e318219deac> (2012).
- Cabrera DeBuc, D. & Somfai, G. M. Early detection of retinal thickness changes in diabetes using optical coherence tomography. *Med. Sci. Monit.* **16**, MT15–MT21 (2010).
- Carpineto, P. *et al.* Neuroretinal alterations in the early stages of diabetic retinopathy in patients with type 2 diabetes mellitus. *Eye (Lond)* **30**, 673–679. <https://doi.org/10.1038/eye.2016.13> (2016).
- Pinilla, I. *et al.* Changes in total and inner retinal thicknesses in type 1 diabetes with no retinopathy after 8 years of follow-up. *Retina* <https://doi.org/10.1097/IAE.0000000000002576> (2019).
- Sohn, E. H. *et al.* Retinal neurodegeneration may precede microvascular changes characteristic of diabetic retinopathy in diabetes mellitus. *Proc. Natl. Acad. Sci. U. S. A.* **113**, E2655–2664. <https://doi.org/10.1073/pnas.1522014113> (2016).
- Early Treatment Diabetic Retinopathy Study Research, G. Photocoagulation for diabetic macular edema. *Arch Ophthalmol* **103**, 1796–1806 (1985).
- Zhu, T., Ma, J., Li, Y. & Zhang, Z. Association between retinal neuronal degeneration and visual function impairment in type 2 diabetic patients without diabetic retinopathy. *Sci. China Life Sci.* **58**, 550–555. <https://doi.org/10.1007/s11427-015-4858-8> (2015).
- Hirai, F. E., Tielsch, J. M., Klein, B. E. K. & Klein, R. Ten-year change in vision-related quality of life in type 1 diabetes: Wisconsin epidemiologic study of diabetic retinopathy. *Ophthalmology* **118**, 353–358 (2011).
- The relationship of glycemic exposure (HbA1c) to the risk of development and progression of retinopathy in the diabetes control and complications trial. *Diabetes* **44**, 968–983 (1995).
- Sun, T. S. & Zhang, M. N. Characters of contrast sensitivity in diabetic patients without diabetic retinopathy. *Zhonghua Yan Ke Za Zhi* **48**, 41–46 (2012).
- Shapley, R. & Hugh Perry, V. Cat and monkey retinal ganglion cells and their visual functional roles. *Trends Neurosci* **9**, 229–235 (1986).
- Barton, F. B., Fong, D. S., Knatterud, G. L. & Group, E. R. Classification of Farnsworth-Munsell 100-hue test results in the early treatment diabetic retinopathy study. *Am J Ophthalmol* **138**, 119–124. <https://doi.org/10.1016/j.ajo.2004.02.009> (2004).
- Utku, D. & Atmaca, L. S. Farnsworth-Munsell 100-hue test for patients with diabetes mellitus. *Ann. Ophthalmol.* **24**, 205–208 (1992).
- Hardy, K. J., Lipton, J., Scase, M. O., Foster, D. H. & Scarpello, J. H. Detection of colour vision abnormalities in uncomplicated type 1 diabetic patients with angiographically normal retinas. *Br. J. Ophthalmol.* **76**, 461–464 (1992).
- Tavares Ferreira, J. *et al.* Retinal neurodegeneration in diabetic patients without diabetic retinopathy. *Investig. Ophthalmol. Vis. Sci.* **57**, 6455–6460 (2016).
- Verma, A. *et al.* Is neuronal dysfunction an early sign of diabetic retinopathy? Microperimetry and spectral domain optical coherence tomography (SD-OCT) study in individuals with diabetes, but no diabetic retinopathy. *Eye (Lond)* **23**, 1824–1830. <https://doi.org/10.1038/eye.2009.184> (2009).
- Ozdek, S. C. *et al.* Optical coherence tomographic assessment of diabetic macular edema: comparison with fluorescein angiographic and clinical findings. *Ophthalmologica* **219**, 86–92. <https://doi.org/10.1159/000083266> (2005).
- Sánchez-Tocino, H., Alvarez-Vidal, A., Maldonado, M. J., Moreno-Montañés, J. & García-Layana, A. Retinal thickness study with optical coherence tomography in patients with diabetes. *Invest. Ophthalmol. Vis. Sci.* **43**, 1588–1594 (2002).
- Gardner, T. W., Antonetti, D. A., Barber, A. J., LaNoue, K. F. & Levison, S. W. Diabetic retinopathy: more than meets the eye. *Surv. Ophthalmol.* **47**(Suppl 2), S253–262 (2002).
- Krogsaa, B., Lund-Andersen, H., Mehlsen, J. & Sestoft, L. Blood-retinal barrier permeability versus diabetes duration and retinal morphology in insulin dependent diabetic patients. *Acta Ophthalmol. (Copenh)* **65**, 686–692 (1987).
- Xu, H. Z. & Le, Y. Z. Significance of outer blood-retina barrier breakdown in diabetes and ischemia. *Invest. Ophthalmol. Vis. Sci.* **52**, 2160–2164. <https://doi.org/10.1167/iovs.10-6518> (2011).

30. Mizutani, M., Kern, T. S. & Lorenzi, M. Accelerated death of retinal microvascular cells in human and experimental diabetic retinopathy. *J. Clin. Invest.* **97**, 2883–2890. <https://doi.org/10.1172/JCI118746> (1996).
31. Barber, A. J. A new view of diabetic retinopathy: a neurodegenerative disease of the eye. *Prog. Neuropsychopharmacol. Biol. Psychiatry* **27**, 283–290. [https://doi.org/10.1016/S0278-5846\(03\)00023-X](https://doi.org/10.1016/S0278-5846(03)00023-X) (2003).
32. Barber, A. J. *et al.* Neural apoptosis in the retina during experimental and human diabetes. Early onset and effect of insulin. *J. Clin. Invest.* **102**, 783–791. <https://doi.org/10.1172/JCI2425> (1998).
33. Mizutani, M., Gerhardinger, C. & Lorenzi, M. Müller cell changes in human diabetic retinopathy. *Diabetes* **47**, 445–449 (1998).
34. Lattanzio, R. *et al.* Macular thickness measured by optical coherence tomography (OCT) in diabetic patients. *Eur. J. Ophthalmol.* **12**, 482–487 (2002).
35. Dhasmana, R., Sah, S. & Gupta, N. Study of retinal nerve fibre layer thickness in patients with diabetes mellitus using Fourier domain optical coherence tomography. *J. Clin. Diagn. Res.* **10**, NC05–NC09. <https://doi.org/10.7860/JCDR/2016/19097.8107> (2016).
36. Bahrami, B. *et al.* Influence of retinal pathology on the reliability of macular thickness measurement: a comparison between optical coherence tomography devices. *Ophthalmic Surg. Lasers Imaging Retina* **48**, 319–325. <https://doi.org/10.3928/23258160-20170329-06> (2017).
37. Tan, C. S., Chan, J. C., Cheong, K. X., Ngo, W. K. & Sadda, S. R. Comparison of retinal thicknesses measured using swept-source and spectral-domain optical coherence tomography devices. *Ophthalmic Surg. Lasers Imaging Retina* **46**, 172–179. <https://doi.org/10.3928/23258160-20150213-23> (2015).
38. Podoleanu, A. G. Optical coherence tomography. *J. Microsc.* **247**, 209–219. <https://doi.org/10.1111/j.1365-2818.2012.03619.x> (2012).
39. Patel, P. J. *et al.* Repeatability of stratus optical coherence tomography measures in neovascular age-related macular degeneration. *Invest. Ophthalmol. Vis. Sci.* **49**, 1084–1088. <https://doi.org/10.1167/iovs.07-1203> (2008).
40. Krebs, I. *et al.* Conversion of Stratus optical coherence tomography (OCT) retinal thickness to Cirrus OCT values in age-related macular degeneration. *Br. J. Ophthalmol.* **95**, 1552–1554. <https://doi.org/10.1136/bjo.2010.194670> (2011).
41. Ciresi, A. *et al.* OCT is not useful for detection of minimal diabetic retinopathy in type 1 diabetes. *Acta Diabetol.* **47**, 259–263. <https://doi.org/10.1007/s00592-010-0193-5> (2010).
42. Park, H. Y., Kim, I. T. & Park, C. K. Early diabetic changes in the nerve fibre layer at the macula detected by spectral domain optical coherence tomography. *Br. J. Ophthalmol.* **95**, 1223–1228. <https://doi.org/10.1136/bjo.2010.191841> (2011).
43. Wolter, J. R. Diabetic retinopathy. *Am. J. Ophthalmol.* **51**, 1123–1141 (1961).
44. van Dijk, H. W. *et al.* Selective loss of inner retinal layer thickness in type 1 diabetic patients with minimal diabetic retinopathy. *Invest. Ophthalmol. Vis. Sci.* **50**, 3404–3409. <https://doi.org/10.1167/iovs.08-3143> (2009).
45. van Dijk, H. W. *et al.* Decreased retinal ganglion cell layer thickness in patients with type 1 diabetes. *Invest. Ophthalmol. Vis. Sci.* **51**, 3660–3665. <https://doi.org/10.1167/iovs.09-5041> (2010).
46. van Dijk, H. W. *et al.* Early neurodegeneration in the retina of type 2 diabetic patients. *Invest. Ophthalmol. Vis. Sci.* **53**, 2715–2719. <https://doi.org/10.1167/iovs.11-8997> (2012).
47. Ng, D. S. *et al.* Retinal ganglion cell neuronal damage in diabetes and diabetic retinopathy. *Clin. Exp. Ophthalmol.* **44**, 243–250. <https://doi.org/10.1111/ceo.12724> (2016).
48. Vujosevic, S. & Midena, E. Retinal layers changes in human preclinical and early clinical diabetic retinopathy support early retinal neuronal and Müller cells alterations. *J. Diabetes Res.* **2013**, 905058. <https://doi.org/10.1155/2013/905058> (2013).
49. Vujosevic, S. *et al.* Early microvascular and neural changes in patients with type 1 and type 2 diabetes mellitus without clinical signs of diabetic retinopathy. *Retina* **39**, 435–445 (2019).
50. Srinivasan, S. *et al.* Retinal tissue thickness in type 1 and type 2 diabetes. *Clin. Exp. Optom.* **99**, 78–83 (2016).
51. Scarinci, F. *et al.* Single retinal layer evaluation in patients with type 1 diabetes with no or early signs of diabetic retinopathy: The first hint of neurovascular crosstalk damage between neurons and capillaries?. *Ophthalmologica* **237**, 223–231 (2017).
52. Barouch, F. C. *et al.* Integrin-mediated neutrophil adhesion and retinal leukostasis in diabetes. *Invest. Ophthalmol. Vis. Sci.* **41**, 1153–1158 (2000).
53. Boeri, D., Maiello, M. & Lorenzi, M. Increased prevalence of microthromboses in retinal capillaries of diabetic individuals. *Diabetes* **50**, 1432–1439 (2001).
54. Gardiner, T. A., Archer, D. B., Curtis, T. M. & Stitt, A. W. Arteriolar involvement in the microvascular lesions of diabetic retinopathy: implications for pathogenesis. *Microcirculation* **14**, 25–38 (2007).
55. Srivastav, K. *et al.* Increased serum level of homocysteine correlates with retinal nerve fiber layer thinning in diabetic retinopathy. *Mol. Vis.* **22**, 1352–1360 (2016).
56. Nadri, G. *et al.* Disorganization of retinal inner layers correlates with ellipsoid zone disruption and retinal nerve fiber layer thinning in diabetic retinopathy. *J. Diabetes Complicat.* **33**, 550–553 (2019).
57. Jain, A., Saxena, S., Khanna, V. K., Shukla, R. K. & Meyer, C. H. Status of serum VEGF and ICAM-1 and its association with external limiting membrane and inner segment-outer segment junction disruption in type 2 diabetes mellitus. *Mol. Vis.* **19**, 1760–1767 (2013).

Acknowledgements

The authors thank the patients in this study and colleges contribution. Publication of this article was supported by the General Council of Aragon (Diputación General de Aragón) Group B08_7R, the Health Research Fund Instituto de Salud Carlos III (Fondo de Investigación Sanitaria, Spanish Ministry of Health) PI13/01124 and PI20/00740 by Fondo Europeo de Desarrollo Regional (FEDER) funds: “Una manera de hacer Europa”, RETICS-Oftared RD16/0008 and Menarini Laboratories. The sponsor or funding organization had no role in the design or conduct of this research.

Author contributions

I.P. and J.A. designed the research. E.O.H. and L.P. recruited the control and diabetic subjects and performed the experiments. A.S.C. and E.O.H. did the statistical calculations, made tables and critically reviewed the manuscript. E.M.L.A. critically reviewed the manuscript for important intellectual content. A.S.C. reviewed the data and the SD-OCT images. I.P. did the eye fundus examinations. I.P. and E.O.H. wrote the manuscript. All authors gave final approval of the version of the manuscript to be submitted and any revised version. The corresponding author attests that all listed authors meet authorship criteria and that no others meeting the criteria have been omitted.

Competing interests

The authors declare no competing interests.

Additional information

Correspondence and requests for materials should be addressed to E.O.-H.

Reprints and permissions information is available at www.nature.com/reprints.

Publisher's note Springer Nature remains neutral with regard to jurisdictional claims in published maps and institutional affiliations.



Open Access This article is licensed under a Creative Commons Attribution 4.0 International License, which permits use, sharing, adaptation, distribution and reproduction in any medium or format, as long as you give appropriate credit to the original author(s) and the source, provide a link to the Creative Commons licence, and indicate if changes were made. The images or other third party material in this article are included in the article's Creative Commons licence, unless indicated otherwise in a credit line to the material. If material is not included in the article's Creative Commons licence and your intended use is not permitted by statutory regulation or exceeds the permitted use, you will need to obtain permission directly from the copyright holder. To view a copy of this licence, visit <http://creativecommons.org/licenses/by/4.0/>.

© The Author(s) 2021